Available at: http://www.ictp.trieste.it/~pub_off IC/99/121

United Nations Educational Scientific and Cultural Organization
and
International Atomic Energy Agency
THE ABDUS SALAM INTERNATIONAL CENTRE FOR THEORETICAL PHYSICS

STOCHASTIC RESONANCE OF THE COUPLED NEURONAL OSCILLATORS

Hyungtae Kook*
Department of Physics, Kyungwon University,
Sungnam, Kyunggi 461-701, Korea
and
The Abdus Salam International Centre for Theoretical Physics,
Trieste, Italy,

Won Sup Kim and Seung Kee Han
Department of Physics, Chungbuk National University,
Cheongju, Chungbuk 361-763, Korea.

Abstract

The stochastic resonance of the coupled neuronal oscillators is studied using the simple model of one-dimensional overdamped oscillators subject to a subthreshold periodic forcing. The stochastic characteristics of the system are shown by the SNR and the cross correlations and its underlying deterministic dynamics are also analyzed which provide an enlightment on the observed stochastic behaviors.

MIRAMARE – TRIESTE

September 1999

*Regular Associate of the Abdus Salam ICTP.

I. INTRODUCTION

The nervous systems of the organisms provide an interesting example of the complex systems. Recently attempts have been made to understand the behaviors of the systems from the viewpoint of the nerve systems as assemblies of the coupled nonlinear oscillators or the oscillator networks, in which temporal dynamics of the constituent neurons are modeled with nonlinear oscillators [1]. As now being considered as a classical work in the neurophysiology, Hodgkin and Huxley had proposed a model neuron that is capable of exhibiting the realistic dynamic characteristics of biological neurons [2]. Various experimental results have also supported the fact that a neuron is a dynamical unit capable of displaying the various characteristics of nonlinear dynamics such as chaos [3].

The recent electrophysiological experiments on the visual cortex have revealed the presence of the oscillatory rhythms in the measurement of the local field potential upon the presentation of moving visual stimuli, whose dynamic behavior of synchronization of the oscillations was shown to be closely related to the underlying mechanism for the visual perceptions [4,5]. It has been also known that the olfactory cortex has an anatomical structure and reveals dynamics similar to the one of an associative memory model. Quite similar oscillatory behaviors including chaos have been observed to arise in the network with an inhibitory feedback loop between the pyramidal cells and the inhibitory interneurons, which has encouraged the speculations on the possible role of chaos in the information processings of the brain [6]. Motivated by the physiological observations mentioned above a variety of the oscillator neural networks has been proposed and studied to find the ways of understanding and predicting the behaviors of the nervous systems [1,6–11].

Meanwhile, noise, which is unavoidable in the real-world environments, has been regarded as an object beyond the scope of a deterministic prediction and has been usually described using statistical methods. As long as its strength is sufficiently weak, the effect of noise is regarded not to be harmful to the otherwise noise-free situations even though its role is still useless. Strikingly, however, it has been recently observed that a noise may play a stunning role and could be utilized in detecting sensory signals that are too weak to be detected otherwise. That is, when a weak subthreshold periodic force is applied to a nonlinear system with a threshold, it has been shown that the signal-to-noise ratio(SNR), which is a measure of the system response, attains a maximal value for an intermediate level of the noise intensity. This optimal performance is obtained when a resonance occurs between the forcing period and the noise-induced time scale of a hopping over the threshold. This phenomenon is referred to as the "stochastic resonance" in the literatures [12,13]. Since its introduction of the idea by Benzi et al. [14] to explain the periodicity of Earth's Ice ages, the stochastic resonance has been studied in a variety of contexts including the ring lasers [15], the electronic circuit [16,17], and the sensory neuronal systems [18–20]. The stochastic resonance has been studied also for the coupled systems and it has been reported that the coupling enhances the stochastic resonance in the arrays of nonlinear oscillators [21].

Both the views of the nervous system as an oscillator network and the active role

of noise in the stochastic resonance encourage an attempt at studying the behaviors of the nervous systems using nonlinear oscillator network models responding to noisy input stimuli. Nevertheless, a systematic understanding of the complex behaviors of the networks is still a formidable task. Prior to attacking the more complex network problems, therefore, it would be useful to gain an insight into the underlying mechanisms for the coupled dynamics using a simple system consisting of a smaller number of coupled oscillators, which becomes rather tractable in analysing the behaviors. Thus, in the present work we consider the two coupled stochastic oscillators. One may expect that the behaviors of the coupled dynamics is underlied by an interplay between the determistic dynamics and the stochastic noise with its active role in the context of the stochastic resonance. The coupled stochastic dynamics is characterized using both the signal-to-noise ratio (SNR) and the cross correlations. The present work focuses on the dependence of those quantities on the coupling strength and the noise intensity. It is observed that the behaviors of the coupled system are related to its underlying deterministic dynamics part of which is viewed in terms of stability of the synchronized states. Related to the present work, recent studies have shown how the stochastic resonance depends on the system parameters such as the forcing period and the amplitude in the bistable systems and the excitable systems as well [22–24]. However, previous studies are mainly for the single oscillators and understandings for the coupled systems are still lacking.

The present paper is organized as follows. The stochastic neuronal oscillator and the coupled system are introduced in section II. The details of the dynamical response of the coupled oscillators against external stimuli with noise are presented in section III. In section IV the underlying deterministic dynamics are analyzed and its implications to the stochastic dynamics are sought. In section V we conclude.

II. STOCHASTIC NEURONAL OSCILLATOR

A neuron subject to a stimulus typically exhibits the 'all-or-none' response. That is, if the stimulus is weak than the neuron in its resting state does not fire and the membrane potential basically remains near the resting state. If the stimulus is strong enough, however, the neuron fires the action potential that has the characteristic size and shape independently of the stimulus. In this paper such an activation of a neuron from the resting state to the firing state is described by a one-dimensional overdamped nonlinear oscillator:

$$\frac{dx}{dt} = -\frac{dU(x)}{dx} + I(t) + \sqrt{2D}\xi, \tag{1}$$

where x represents the membrane voltage and the potential function is given as $U(x) = -1/2x^2 + 1/4x^4$. The potential has a barrier at $x = 0$ which plays the role of the crossover threshold between two minima; the minima are regarded as the resting state (the left minimum) and the firing state (the right minimum) of the neuron. For a real neuron the firing state usually lasts only for a brief period and is followed by an inactivation

process restoring the membrane potential back to the resting state. This mechanism of the inactivation is introduced in our model by holding the activation variable x for a brief time and then resetting it to $x = x_0$ whenever x reaches a prescribed value x_m; x_m and x_0 in each minima can be chosen arbitrarily since their precise values do not lead to an appreciable change in the results. We set $x_m = 0.9$ and $x_0 = -2.0$ in the present work.

The model can be regarded as a further simplified version of the more realistic models such as the Hodgkin-Huxley [2], the Morris-Lecar [25], or the Fitzhugh-Nagumo [26,27] neuron models. The simplification to the one-dimensional oscillator model greatly reduces the computation complexity of the coupled neural oscillators system.

In the equation $I(t)$ represents the periodic driving force $I(t) = I_0 \sin(\omega_0 t)$: we set $\omega_0 = 0.1$. When the strength of stimulus I_0 is larger than the threshold value, $I_{th} \sim 0.42$, the model neuron exhibits sustained periodic firings. When the input stimulus is below the threshold value, x cannot reach the firing state and just wobbles around the resting state. In the present work, if not specified otherwise, the input stimulus is assumed to be at the subthreshold regime, $I_0 = 0.36$, so that the input forcing does not suffice to excite the neuron by itself. However, in the presence of noise, as added in the last term of Eq. (1), the model neuron can be driven to the firing regime even with the subthreshold $I(t)$ stimuli; D is the noise intensity and ξ is the guassian white noise defined as

$$\langle \xi(t) \rangle = 0, \ \langle \xi(t)\xi(t') \rangle = \delta_{t,t'}. \tag{2}$$

As one tunes the level of the noise intensity, the system exhibits the well known behavior of the stochastic resonance. That is, the SNR of the system response at the driving frequency ω_0 attains its optimum at a certain intermediate level of the noise. The stochastic resonance arises due to a resonance between the noise-induced time scale of the hopping across the threshold and the forcing period. More details observed for the stochastic resonance can be found elsewhere [11–13].

Now, let us introduce the coupled system as follows:

$$\begin{aligned} \frac{dx_1}{dt} &= -\frac{dU(x_1)}{dx_1} + I_1(t) + \sqrt{2D}\xi_1 + \gamma_1(x_2 - x_1) \\ \frac{dx_2}{dt} &= -\frac{dU(x_2)}{dx_2} + I_2(t) + \sqrt{2D}\xi_2 + \gamma_2(x_1 - x_2), \end{aligned} \tag{3}$$

where the white noises ξ_1 and ξ_2 to each oscillator are uncorrelated, that is, $\langle \xi_1(t)\xi_2(t') \rangle = 0$. The input currents $I_1(t)$ and $I_2(t)$ are set to be identical. The coupling constants γ_1 and γ_2 can be either positive or negative; the attractive force ($\gamma > 0$) and the repulsive force ($\gamma < 0$) typically lead to an excitatory and an inhibitory coupling, respectively. To understand the cooperative behavior between two oscillations under coupling of different nature, we consider in the followings the two cases: a) the mutual excitatory coupling $\gamma_1 = \gamma_2 = \gamma > 0$, and b) the mutual inhibitory coupling $\gamma_1 = \gamma_2 = \gamma < 0$.

In Fig's. 1, the temporal activities of the two oscillators are shown for each case of coupling. In each figure the firing events of the oscillators are depicted in the upper two plots. The sinusoidal graph at the bottom denotes the common periodic driving force. The long vertical line across the graphs denotes the moment when the coupling is turned

on. As one can see from these figures, two oscillations are strongly synchronized for the excitatory coupling case (Fig. 1(a)) and strongly desynchronized for the inhibitory coupling case (Fig. 1(b)) as soon as the coupling is turned on. That is, the excitatory coupling typically induces synchrony between two oscillations, whereas the inhibitory coupling induces desynchrony. One may also notice a certain amount of synchrony present even before the coupling is turned on, which is only due to the common driving force.

III. STOCHASTIC RESONANCE OF THE TWO COUPLED OSCILLATORS

To see the firing response of the coupled oscillators to noise, the SNR for each coupling case has been estimated. The SNR varies depending on the coupling strength as well as the noise intensity as shown in Fig. 2. For the excitatory coupling case, as shown in Fig. 2(a), the SNR at weaker noise intensities ($D < D_0$) is reduced whereas it is enhanced at larger noise intensities ($D > D_0$) when compared to the single uncoupled oscillator case; $D_0 \sim 0.1$ is the optimal noise intensity for the single oscillator [11]. This is due to the attractive force between two phases of oscillations, originating from the nature of the excitatory coupling. Enhancement of the SNR due to the excitatory coupling has been previously reported for coupled oscillator systems [21,28,29].

The mechanism for the coupling dependence of the SNR can be viewed in the level of the neuronal activity as follows. The excitatory coupling tends to reduce the phase difference of two oscillators. At a weak noise intensity, both oscillators have less chance of firings and hence it is more likely that they are in the resting state. Suppose now that the phase of one oscillator manages to get closer to the threshold and is ready to fire. The oscillator would fire only if a sufficiently strong noise kick occurs on it. However, the amount of noise should be larger than the uncoupled oscillator case since the oscillator, now coupled, should overcome the attraction from the other oscillator at the resting state in addition to the pulling force by the nonlinear potential $U(x)$. Therefore, it is more likely that the firing of the oscillator is suppressed and, consequently, the firing rate is reduced compared to the single oscillator case. Furthermore, this effect is evidently enhanced as the coupling becomes stronger. On the other hand, when the noise intensity is large ($D > D_0$) both oscillators have more chance to be in the firing state. Even when one oscillator is yet in the resting state the other oscillator in the firing state attracts the oscillator and helps firing. Consequently, the SNR will be enhanced and this effect also becomes enhanced as the coupling is stronger.

A quite different mechanism applies to the inhibitory coupling case since the nature of the coupling now introduces the repulsive force instead of the attractive force.(See Fig. 2(b)) It is noticeable that the change of the SNR for the inhibitory coupling case is much more prominent, especially in the weak noise regime, compared to the excitatory coupling case. This results mainly from the nature of inhibitory coupling that enhances the coupling strength effectively. Namely, with the excitatory coupling a small deviation of two oscillating phases tends to decrease and the effective coupling between two oscillators becomes smaller as a result. Meanwhile, the deviation tends to increase for the inhibitory

coupling case due to the repulsive force and, therefore, the effective coupling becomes larger. The increase of the effective coupling strength for the inhibitory coupling case can thus lead to a nontrivial result in the coupled oscillations, unlike for the excitatory coupling case.

In fact, besides the noise and the driving force, the effective force between the coupled oscillations comes from the combined effect of the potential $U(x)$ and the coupling. Near the left minimum of the potential (the resting state) the potential gradient tends to synchronize the oscillations, while it tends to desynchronize the oscillations near the threshold because of the reversed curvature of the potential. Therefore, in a simplified picture, one may describe a typical firing of oscillators with inhibitory coupling in the following three steps:

1. a periodic approach of both oscillators to the threshold driven by input force,
2. a small deviation in phase due to noise, and then
3. a mutual repulsion of the phases due to the combined effect of the potential gradient and the inhibitory coupling.

In step 2, the order of the phases is randomly selected by noise and the oscillator of the advanced phase will be finally led to fire by the repulsive force of step 3, whereas the other oscillator of the lagged phase is pushed back to the resting state. More detailed analysis on the combined effect of the potential and the coupling will be given in the following section.

The observation of the enhanced SNR at the weak noise intensity due to the inhibitory coupling is very important for the purpose of the segmentation performance of the oscillator network since this implies the increased average firing rate of neurons [11].

The degree of coherency between two oscillations is measured by the cross correlations defined as follow.

$$C = \frac{1}{N}\sum_{k=1}^{k=N} b_1(kT) \wedge b_2(kT),$$
$$C_A = \frac{1}{N}\sum_{k=1}^{k=N} b_1(kT) \oplus b_2(kT) \tag{4}$$

where T is the period of the input forcing, $T = 2\pi/\omega_0$, and b_i is the binary representation of the activation variable; $b_i = 0$ for $x < 0$ and $b_i = 1$ for $x > 0$. $b_i(kT)$ is measured at the k-th peak of the input forcing within the time window of finite width δ centered around the peak. The operations '$\wedge$' and '$\oplus$' denote the binary operations 'AND' and 'Exclusive OR', respectively. The degree of correlation is estimated using both measures since either measure alone does not properly estimate two kinds of correlations of interest, synchrony and desynchrony, simultaneously over a wide range of the noise intensity. The cross correlation C measures the degree of synchrony, i.e., the occurrences of synchronous firings of two oscillators at the peaks of the input forcing, while the anticorrelation C_A measures the degree of desynchrony. Note that two measures are independent in definition

and that the proposed definitions are different from the conventional ones. However, it is expected that these measures are more natural for the present purpose in that they measure correlations of the firing events only at the input forcing periods.

Fig. 3 shows that the correlations between two oscillations vary depending on the noise intensity as well as on the coupling strength. When the noise intensity is sufficiently weak, the oscillators hardly fire and hence the correlations would be almost zero. As the noise intensity increases, firings start to occur and the magnitudes of both correlations rise due to the coupling between two oscillations. Note that the effect of the inhibitory coupling is more prominent compared to that of the excitatory coupling, especially in the weak noise regime. The inhibitory coupling induces strong anticorrelation at much lower level of the noise intensity. This is, as pointed out above, due to the fact that repulsion of oscillations originating from the inhibitory coupling becomes enlarged at the weak noise level below D_0. Note also that the anticorrelation attains its maximal value at the noise intensity which is much lower compared to the peak position of the SNR curve. It is also observed that the peak shifts to the lower level of noise intensity as the coupling strength increases, which implies the important role of the inhibitory coupling at the low level of the noise intensity.

As the noise intensity becomes too strong beyond D_0, the magnitude of the cross correlations becomes small since the firing of each oscillator is now dominated by the uncorrelated noise ξ_1, ξ_2 and thereby the firings of two oscillators start to be uncorrelated. In fact, this behavior at the high noise level is not reflected properly with the present definition of the cross correlation (Fig. 3(a)) which is supposed to be saturated at the higher level of noise intensity. That is, as the noise intensity increases, the oscillators tend to fire at most of the input forcing periods and this will in turn make the cross correlation saturate even though firings in the whole time range is uncorrelated on average. However, this should not lead to confusions since this behavior can be correctly recognized from the SNR data. Therefore, to understand more properly the cooperative behavior of the coupled oscillations it is necessary to examine both measures of the SNR and the cross correlations.

IV. DETERMINISTIC DYNAMICS ANALYSIS

The stochastic behaviors observed in the previous section are in part a reflection of the underlying deterministic dynamics. In this section, therefore, we examine the deterministic dynamics for Eq. (3) and show its relation to the stochastic behaviors of the previous section.

First, we introduce a coordinate transformation $X = \frac{x+y}{2}$ and $Y = \frac{x-y}{2}$, or equivalently, $x = X + Y$ and $y = X - Y$. It turns out that the new coordinate system is useful in describing the coupled dynamics in a collective way: X represents the center of phase of the oscillations and Y represents the phase difference. Especially, the solution satisfying $Y = 0$ corresponds to the synchronized oscillations. In the new coordinate system, Eq. (3) is transformed into

$$\frac{dX}{dt} = X(1 - X^2 - 3Y^2) + I(t),$$
$$\frac{dY}{dt} = Y\{1 - 4\gamma - (3X^2 + Y^2)\}. \quad (5)$$

Notice that the X equation in Eq. (5) is independent of coupling and also that X is always driven by the periodic force; there is no fixed point of X. Meanwhile, the Y-dynamics is autonomous and $Y = 0$ is the fixed point of Y regardless of the X value; the line $Y = 0$ is an invariant line in the XY phase plane. The second factor of the r.h.s. of the Y equation does not give any further fixed points because X always varies in time. Therefore, in the followings we will focus on the stability of the synchronized states on the invariant line. The dynamics on the invariant line is given by the X equation as follows:

$$\frac{dX}{dt} = X(1 - X^2) + I(t), \quad (6)$$

which is just the same as the single oscillator equation, Eq. (1).

The linear stability of a synchronized state across the invariant line is determined by the sign of $A \equiv 1 - 4\gamma - 3X^2$; stable when $A > 0$ (the nearby trajectories are attracted toward the line $Y = 0$) and unstable when $A < 0$ (the nearby trajectories are repelled away from the line $Y = 0$). In turn, the sign of A is determined by the values of both γ and X. The possible cases can be classified as follows:

1. When $\gamma \geq \frac{1}{4}$:
   $A \leq 0$ is satisfied for all the range of X. The case of $A = 0$ implies the marginal stability. However, this occurs only instantaneously when $X = 0$. Therefore, $Y = 0$ (the synchronized state) is always stable.

2. When $\gamma < \frac{1}{4}$:
   This provides the necessary condition for the existence of the unstable synchrony. The case can be further divided into two subcases.

   (a) $3X^2 > 1 - 4\gamma$ case: $A < 0$ and $Y = 0$ is stable.

   (b) $3X^2 < 1 - 4\gamma$ case: $A > 0$ and $Y = 0$ is unstable.

Therefore, when $\gamma \geq \frac{1}{4}$, the synchronized states are always stable for the whole range of X. However, the synchronized state is unstable when the both conditions of $\gamma < \frac{1}{4}$ and $-\sqrt{\frac{1-4\gamma}{3}} < X < \sqrt{\frac{1-4\gamma}{3}}$ are satisfied. That is, when $\gamma < \frac{1}{4}$, the condition 2(b) implies the existence of a repelling region in X where a small deviation between two phases tends to diverge. This divergence is a direct consequency of the convexity of the potential function around $X = 0$. The region of repelling where $U(X)$ is convex is depicted in Fig. 4. Evidently, the repelling region still exists even when there is no coupling ($\gamma = 0$). Namely, while the repulsive interaction of two oscillations derives from the combined effect of the (repulsive) coupling and the convexity of the potential, the repulsion at $\gamma = 0$ is purely due to the latter effect. It is interesting to find that the region in the presence of the coupling is altered in a way that is specified as in the condition 2(b). That is, the

range of the repelling region changes even though the convexity of the potential does not change: as γ increases from zero the range of repelling shrinks until it completely vanishes at $\gamma = \frac{1}{4}$.

One may notice at this point that the notion of the coupling nature is somewhat misleading. That is, positive γ does not mean that two oscillations are always excitatory and the negative γ does not mean that they are always inhibitory either. We have already seen such a contradictory example as the above condition 2(b) implies that a positive γ for $0 < \gamma < \frac{1}{4}$ may induce a mutual repulsion depending on the oscillation phases, which is the sense of the inhibition. However, we think that the notion is still intuitive even though we should admit that there is no precise correspondance between the sign of γ and the nature of the coupling.

Now, let us look in the nonlinear aspect of dynamics when Y does not remain near the invariant line $Y = 0$. Then one should resort to the original equation, Eq. (5) instead of Eq. (6). Let's consider the equation in a slightly different arrangement:

$$\frac{dX}{dt} = (1 - 3Y^2)X - X^3 + I(t). \tag{7}$$

And attempt to follow the instantaneous change of the potential while neglecting the effect of the periodic force for the moment. Notice that unlike the case of Eq. (6), the equation is now dependent on Y. Let us denote the coefficient of the linear term of Eq. (7) as $B \equiv 1 - 3Y^2$. Suppose both X and Y are small initially: $X = \delta X$ and $Y = \delta Y$. While Y is small yet, B is positive and the potential is of the double-well shape as depicted in Fig. 5(a) when $|Y| < \frac{1}{\sqrt{3}}$. Then, since $X = 0$ is unstable the potential gradient pushes X away from $X = 0$ toward the right minimum of the potential. However, due to the convex potential near $X = 0$, Y also gets large. When Y becomes large enough ($|Y| > \frac{1}{\sqrt{3}}$) the potential loses the structure of the double well and the unstable equilibrium at $X = 0$ bifurcates to the stable one as depicted in Fig. 5(b). Consequently, X is now attracted back toward $X = 0$. Now, if the consideration for $I(t)$ is added to the above one can imagine of more complex behaviors that can arise depending on its phase and the frequency as well.

Similarly, the Y equation can be rewritten as

$$\frac{dY}{dt} = (1 - 4\gamma - 3X^2)Y - Y^3. \tag{8}$$

When $\gamma \geq \frac{1}{4}$, the coefficient of the linear term in Eq. (8) is always negative for all range of X. The potential $U(Y)$ just looks like the Fig. 6(b) and thus the synchronized state of $Y = 0$ is the unique stable state. But when $\gamma < \frac{1}{4}$, the potential changes its shape depending on X. That is, when $3X^2 < 1 - 4\gamma$, the potential is of the double-well shape with two minima at $Y = \pm\sqrt{A}$ and the synchronized state at $Y = 0$ is unstable. Meanwhile, when $3X^2 > 1 - 4\gamma$ as X increases, the local maximum at $Y = 0$ becomes a global minimum, and thus the synchronized state becomes a unique stable state. The change of $U(Y)$ as X is depicted in Fig. 6.

Let us now take a speculative view to a combined dynamics of X and Y in the context of neuronal behaviors. Also let us consider the effect of $I(t)$ and noise together. The case

of $\gamma \geq \frac{1}{4}$ is rather trivial. That is, the synchronized state is stable and two oscillations remain synchronized over all range of X however they are driven by $I(t)$. Therefore, let us consider the other case of $\gamma < \frac{1}{4}$. Assume that both oscillators are initially near the resting state with a small amount of phase difference probably induced by noise: $X \sim -1$ and $Y = \delta Y$. As long as X remains near the resting state (large value of X) Y remains to be small since $Y = 0$ is stable (Fig. 6(b)). However, if X moves toward the threshold driven by $I(t)$ and/or noise, $U(Y)$ changes the shape for small X and the $Y = 0$ becomes unstable (Fig. 6(a)). Then, Y increases. Unless Y becomes too large, X keeps increasing with the aid of the potential gradient (Fig. 5(a)) and probably also of $I(t)$. When Y becomes large enough ($\sim \frac{1}{\sqrt{3}}$), the potential $U(X)$ becomes concave (Fig. 5(b)) and the center of phase moves back to the thershold. The last step does not really play a role in our case since there is the reset mechanism which brings the oscillator back to the resting state once it has fired.

In the case of the subthreshold forcing as we are mainly concerned about in the present work we can think of the role of coupling as follows. For the excitatory coupling ($\gamma \geq \frac{1}{4}$ more precisely), each oscillator has a chance of firing when it is kicked by noise when it is driven near the threshold by $I(t)$. However, they tend to be synchronized as we saw above and, therefore, to be bound, which implies that a larger impact of noise kick on average would be required, as described in detail in section III. This explains the reduction of SNR in the low noise intensity as shown in Fig. 2(a).

For the inhibitory coupling, the oscillators tend to be synchronized when they are near the resting state. However, once they are driven to the repelling region of Fig. 4 they diverge. Then, this divergence, in turn, induces the one oscillator to fire with the aid of the other's repulsion which is itself repelled to the resting state. Therefore, a small amount of noise kick may suffice to lead firing. As the inhibition gets stronger even smaller amount of noise would suffice since the range of the repelling region of Fig. 4 extends as the condition 2(b) above implies. This explains not just the enhancement of the SNR in the low noise intensity as shown in Fig. 2(b), but one can also notice, compared to the effect of the excitatory coupling, that the inhibitory coupling is even more effective especially in the low noise intensity regime. The enhanced cross anticorrelation of Fig. 3(b) in the low noise intensity also reflects the firing activities of the oscillators that are enhanced due to the inhibitory repulsion.

V. CONCLUSIONS

The stochastic resonance of the coupled neuronal oscillators is studied using the simple one-dimensional overdamped oscillators. The stochastic behaviors of the system are characterized with the SNR and the cross correlations.

The excitatory(inhibitory) coupling induces synchrony(desynchrony) between stochastic nonlinear oscillators. But unlike the deterministic case, the degree of correlation depends on the noise intensity as well as on the coupling strength. Also the firing rate of the coupled oscillator, the SNR, shows a strong dependence on both quantities. Especially,

the effect of the inhibitory coupling is prominent at the regime of the low noise intensity.

The deterministic part of the coupled dynamics is analyzed to examine the role of the deterministic dynamics that may underlie the observed stochastic behaviors. It is found that the stability of the synchronized states and the dynamic changes of the potential functions are closely related to the variations of the SNR and the cross correlations of the coupled stochastic oscillators. Especially, one is able to get an intuitive understanding on the enhancement of the SNR and the cross anticorrelation as well at the regime of the low noise intensity.

While concentrated on the simple systems consisting of only a small number of the coupled nonlinear oscillators, the present work still provides fundamental understandings on the coupled stochastic nonlinear oscillators and some insights into the behaviors of more complex systems.

ACKNOWLEDGMENTS

The authors would like to thank Prof. S. Kim for useful discussions. The present work has been supported by the Brain Research Project of the Ministry of Science and Technology of Korea. This work was done within the framework of the Associateship Scheme of the Abdus Salam International Centre for Theoretical Physics, Trieste, Italy. H. K. is thankful for the support of the ICTP for his visit during which the part of the present work was done.

REFERENCES

[1] H. G. Schuster, *Nonlinear Dynamics and Neuronal Networks* (VCH, New York, 1991).

[2] A. L. Hodgkin and A. F. Huxley, J. Physiol. (London) **117**, 117 (1952).

[3] M. A. Arbib., *The Handbook of Brain Theory and Neural Networks*, (MIT Press., Cambridge, 1995).

[4] C. M. Gray, P. König, A. K. Engel, and W. Singer, Nature **338**, 334 (1989).

[5] R. Eckhorn et al., Biol. Cybern. **60**, 121 (1988).

[6] W. J. Freeman, Biol. Cybern., **56**, 139-150, 1987.

[7] D. Horn and M. Usher, Phys. Rev. A **40**, 1036 (1989).

[8] C. Koch and I. Segev, *Methods in Neuronal Modeling*, (MIT Press, Cambridge, 1989).

[9] D. L. Wang, J. M. Buhmann, and C. von der Malsburg, Neural Comp. **2**, 94 (1990).

[10] D. Hansel and H. Sompolinsky, Phys. Rev. Lett. **68**, 718, 1992.

[11] S.K. Han, W.S. Kim, and H. Kook, Phys. Rev. E **58**, 2325 (1998).

[12] K. Wiesenfeld and F. Moss, Nature **373**, 33 (1995).

[13] L. Gammaitoni *et al.*, Phys. Rev. Lett. **74**, 1052 (1995).

[14] R. Benzi, A. Sutera, and A. Vulpiani, J. Phys. A **14**, L453 (1981).

[15] B. McNamara, K. Wiesenfeld, and R. Roy, Phys. Rev. Lett. **60**, 2626 (1988).

[16] L. Gammaitoni *et al.*, Phys. Rev. Lett. **62**, 349 (1989).

[17] M. Dykman *et al.*, Phys. Rev. Lett. **65**, 2606 (1990).

[18] A. Longtin, A. Bulsara, and F. Moss, Phys. Rev. Lett. **67**, 656 (1991).

[19] J. K. Douglass, L. Wilkens, E. Pantazelou, and F. Moss, Nature **365**, 337 (1993).

[20] I. Peterson, Science **144**, 271 (1993).

[21] J. F. Linder, B. K. Meadows, W. L. Ditto, M. E. Inchiosa, and A. R. Bulsara, Phys. Rev. Lett. **75**, 3 (1995).

[22] P. Jung and P. Hanggi, Phys. Rev. A **44**, 8032 (1991).

[23] A. Longtin and D. R. Chialvo, Phys. Rev. Lett. **81**, 4012, 1998.

[24] S.-G. Lee and S. Kim, Phys. Rev. E. **60**, 826, 1999.

[25] C. Morris and H. Lecar, Biophys. J. **35**, 193 (1981).

[26] R. A. Fitzhugh, Biophys. J. , 445 (1961).

[27] J. Nagumo, S. Arimoto, and S. Yoshizawa, Proc. IRE **50**, 2061-2070 (1962).

[28] A. Neiman and L. Schimansky-Geier, Phys. Lett. A **197**, 379 (1995).

[29] M. E. Inchiosa and A. R. Bulsara, Phys. Lett. A **24**, 183 (1995).

(a)

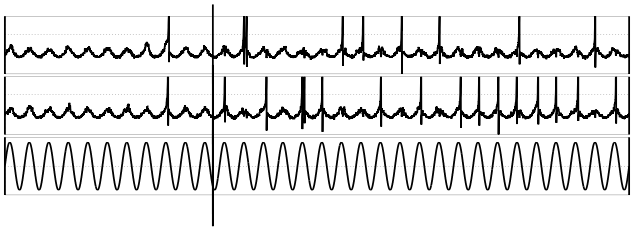

(b)

FIG. 1. Temporal activities of two coupled oscillators. The common sinusoidal forcing is depicted at the bottom of the plots. The long vertical bar across the graphs denotes the moment when the coupling is turned on. (a) The excitatory coupling ($\gamma = 0.3$, $D = 0.02$), and (b) the inhibitory coupling case ($\gamma = -0.3$, $D = 0.004$).

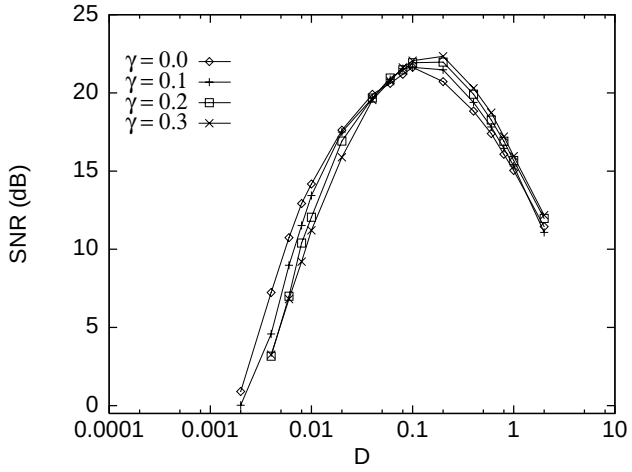

(a)

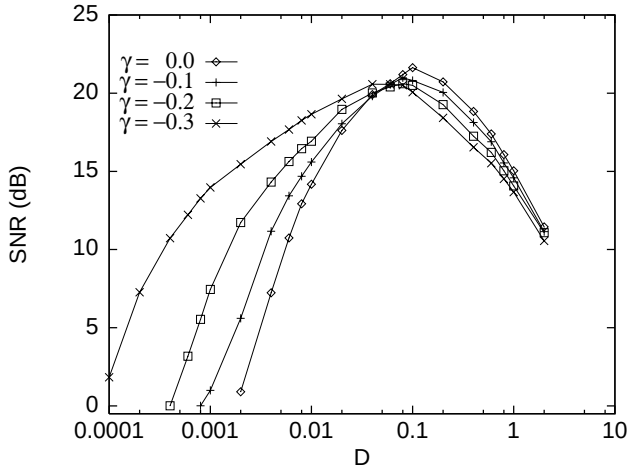

(b)

FIG. 2. SNR for two coupled oscillators with respect to the noise intensity for various magnitudes of the coupling strength: (a)the excitatory coupling and (b)the inhibitory coupling cases.

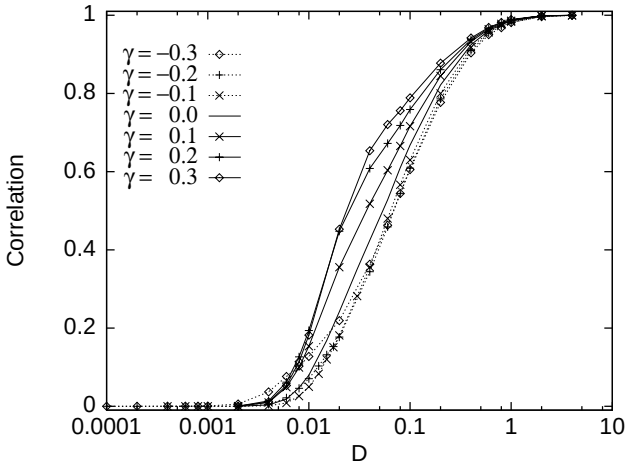

(a)

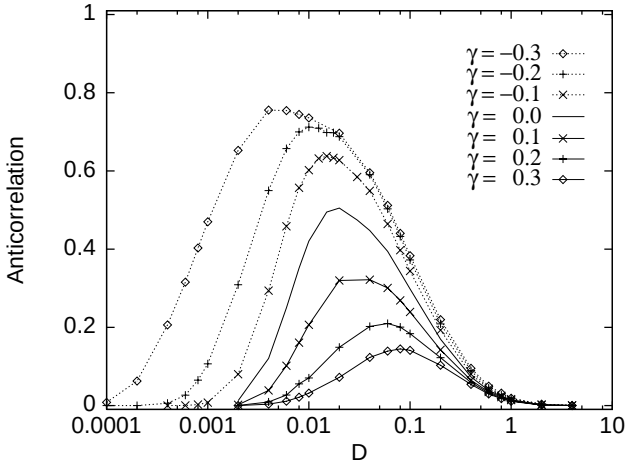

(b)

FIG. 3. Cross correlations between two coupled oscillations with respect to the noise intensity for various magnitudes of the coupling strength: (a)the cross correlation C and (b)the cross anticorrelation C_A.

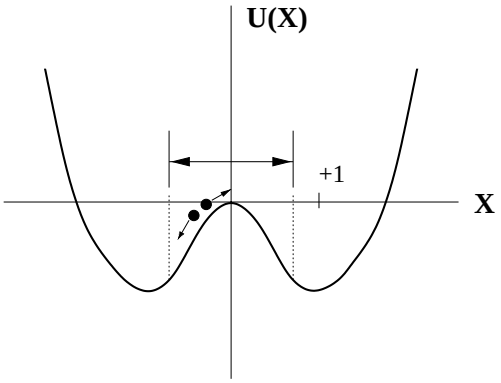

FIG. 4. Repelling region. For $\gamma < \frac{1}{4}$, the designated region represents the range $-\frac{1-4\gamma}{3} < X < \frac{1-4\gamma}{3}$. Within this region two oscillations diverge as schematized by the diverging two solid balls denoting each oscilllator's phase.

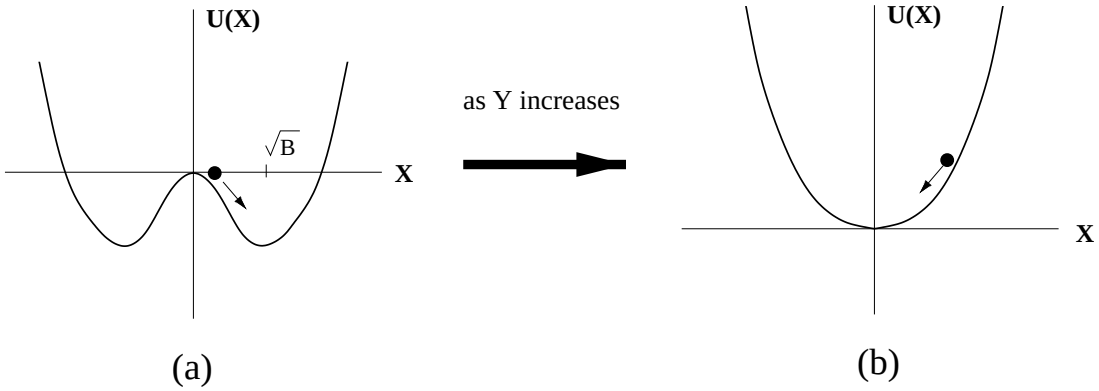

FIG. 5. Change of the potential $U(X)$. (a) When $|Y|$ is small, $|Y| < \frac{1}{\sqrt{3}}$, the potential has the double-well shape and the $X = 0$ is unstable. (b) As Y increases, $X = 0$ becomes a global minimum. The solid ball denotes the center of phase of two oscillators.

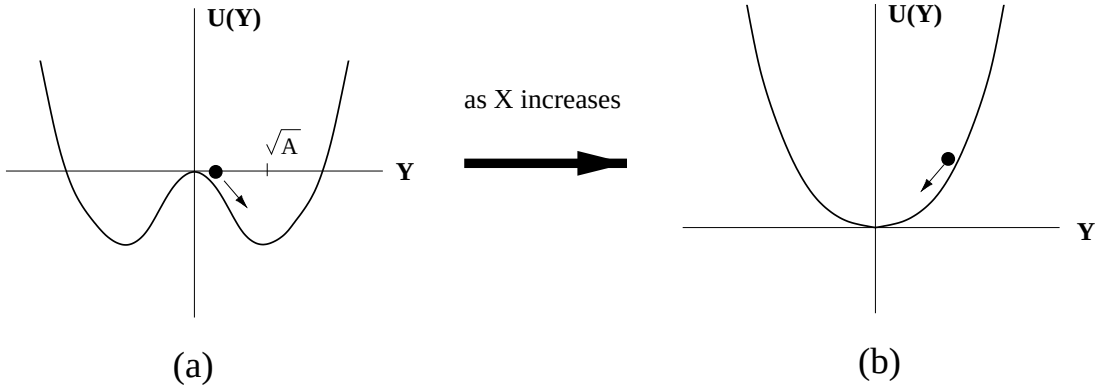

FIG. 6. Change of the potential $U(Y)$. (a) When $\gamma < \frac{1}{4}$ and $3X^2 < 1-4\gamma$, $Y = 0$ is unstable. (b) When X increases and $3X^2 > 1 - 4\gamma$, $Y = 0$ is globally stable. The solid ball represents the phase difference of the two oscillators. For $\gamma > \frac{1}{4}$, $U(Y)$ looks the same as (b).